

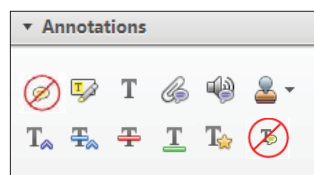
## Page Proof Instructions and Queries

**Journal Title:** MMS  
**Article Number:** 637234

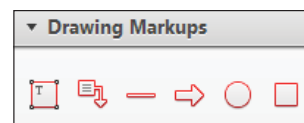
Greetings, and thank you for publishing with SAGE. We have prepared this page proof for your review. Please respond to each of the below queries by digitally marking this PDF using Adobe Reader.

Click “Comment” in the upper right corner of Adobe Reader to access the mark-up tools as follows:

For textual edits, please use the “Annotations” tools. Please refrain from using the two tools crossed out below, as data loss can occur when using these tools.



For formatting requests, questions, or other complicated changes, please insert a comment using “Drawing Markups.”




Detailed annotation guidelines can be viewed at: <http://www.sagepub.com/repository/binaries/pdfs/AnnotationGuidelines.pdf>  
 Adobe Reader can be downloaded (free) at: <http://www.adobe.com/products/reader.html>.

Sl. No.	Query
---------	-------

- |   |   |
|---|---|
| 1 | AQ: Please check that the author, affiliation and corresponding author details are as intended. |
| 2 | AQ: Please check that the missing closing bracket in this sentence has been placed as intended. |
| 3 | AQ: Please provide descriptions for parts Figure 1 (a) and (b).                                 |
| 4 | AQ: Please provide descriptions for Figure 2 parts (a) and (b).                                 |
| 5 | AQ: “Figure 11” changed to “Figure 15” here – OK?   |
| 6 | AQ: All cos, sin, sqrt, etc. have been changed to lower case. Please confirm this is correct.   |
| 7 | AQ: Please check that the funding statement is appropriate.                                     |
| 8 | AQ: Ref 18: Please give the city of publication.  |

# A new approach for the determination of the global minimum time for the Chaplygin sleigh brachistochrone problem

Mathematics and Mechanics of Solids  
1–21  
© The Author(s) 2016  
Reprints and permissions:  
sagepub.co.uk/journalsPermissions.nav  
DOI: 10.1177/1081286516637234  
mms.sagepub.com  


**R Radulović**

*Faculty of Mechanical Engineering, University of Belgrade, Serbia*

**S Šalinić**

*Faculty of Mechanical Engineering, University of Kragujevac, Serbia*

**A Obradović**

*Faculty of Mechanical Engineering, University of Belgrade, Serbia*

**S Rusov**

*Faculty of Transport and Traffic Engineering, University of Belgrade, Serbia*

Received 4 June 2015; accepted 12 February 2016

## Abstract

A new approach for the determination of the global minimum time for the case of the brachistochronic motion of the Chaplygin sleigh is presented. The new approach is based on the use of the shooting method in solving the corresponding two-point boundary-value problem and defining either the crossing points of surfaces or the crossing points space of curves in a three-dimensional space of two costate variables and the time of the brachistochronic motion of the sleigh. A number of examples for multiple extremals of the Chaplygin sleigh brachistochrone problem are provided. In these examples, the global minimum is the solution to which the minimum time of motion corresponds.

## Keywords

Global minimum time, Chaplygin sleigh, brachistochrone, Pontryagin's maximum principle, optimal control

## 1. Introduction

In Jeremić et al. [1] and Šalinić et al. [2,3], considerations of the brachistochronic motion of a particle involve the application of the shooting method [4] in solving a corresponding two-point boundary-value problem (TPBVP). The shooting method in these papers is reduced to solving a corresponding system of nonlinear algebraic equations, where the unknowns are values of some state and costate variables at characteristic instants. Depending on the number of unknowns, the solution of the considered system of algebraic equations could be geometrically represented in the form of intersection of the corresponding surfaces or hypersurfaces.

---

### Corresponding author:

S Šalinić, University of Kragujevac, Dositejeva 19, Kraljevo, 36000, Serbia.  
Email: salinic.s@ptt.rs

Obradović et al. [5] consider a general case of brachistochronic motion of the rheonomic mechanical system with linear rheonomic nonholonomic constraints, a sledge moving along a horizontal block of ice being taken as an example, and its law of motion is known. The considered paper introduces a single control, and the TPBVP is reduced to solving a four-parameter shooting, where it is not possible to claim with certainty that the obtained solution is optimal if it is taken into account that there is not a general procedure for determining all possible solutions of the TPBVP in a four-parameter shooting. The final value of the sledge angle was  $\pi/4$ . Radulović et al. [6] consider the brachistochronic motion of the mechanical system with a nonlinear nonholonomic constraint. In the considered work, the particles, with the imposed constrained motion in the form of perpendicularity of velocities by means of two Chaplygin knife edges, are connected by a light mechanism. The brachistochrone problem is formulated as a task of optimal control by introducing two controls, where the TPBVP is also reduced in this case to solving a four-parameter shooting, where it was not possible to estimate the interval of values of the unknown quantities  $\lambda_x$  and  $\lambda_y$ .

In the present paper, a visual representation of the TPBVP is used to explore the possibility of multiple extremal occurrence in the problem of the brachistochronic motion of the Chaplygin sleigh considered by Šalinić et al. [7]. In the case of multiple extremals the choice corresponds with the extremals to which the minimum time of brachistochronic motion corresponds. The process of defining the number of possible extremals and defining the extremal to which the minimum time of motion corresponds will be henceforth referred to as the determination of the global minimum time.

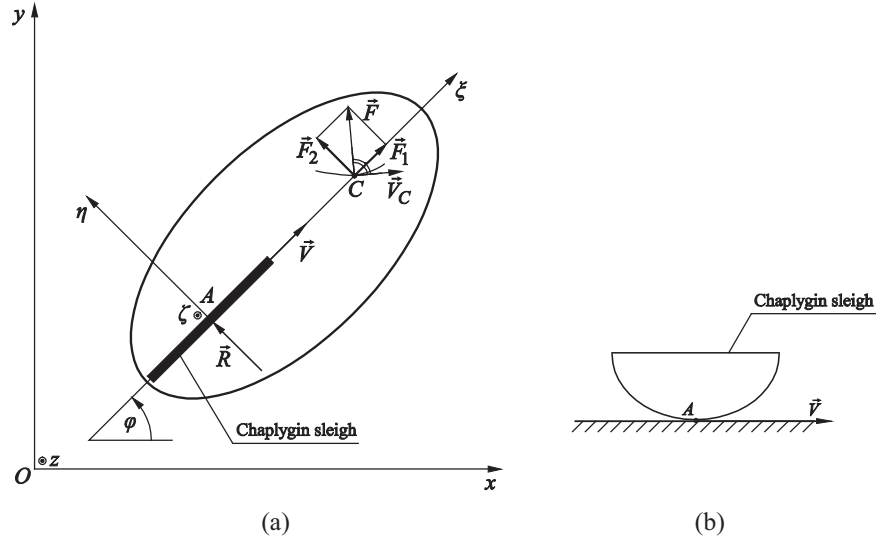
Taking into account that it is not possible to provide a general procedure for estimating the interval of values of the missing parameters when solving the TPBVP in the brachistochronic motion of nonholonomic mechanical systems with arbitrary initial and final position, nor is there a theorem on the existence and uniqueness of the TPBVP solution, it makes sense to raise the following questions not considered by Šalinić et al. [7]: Is there at all the solution of a corresponding TPBVP at known initial and final position of the Chaplygin sleigh? Is it possible to estimate the interval of values of the missing parameters? Is there a procedure for determining all possible solutions of the TPBVP? The significance of the above questions, so that it can be claimed with certainty that a solution of the TPBVP exists and that the obtained solution is optimal too, motivated the authors to write the present paper.

Now, we can refer to the technical application of the results obtained within the framework of this paper, with the possibility of real application. The obtained results, on one hand, can be applied to the problems of determining optimal motion of nonholonomic mechanical systems (not only to determining optimal motion of the Chaplygin sleigh, but also to all nonholonomic mechanical systems described by the same equations of state, such as the simplified vehicle model presented by Radulović et al. [8]), as well as in vertical rolling of a disk without slipping (see Bloch [9]), with a technical requirement posed in the form of determining the optimal trajectory of motion, so that the considered nonholonomic mechanical system moves from a known initial position to a final defined position in a minimum time. On the other hand, the results obtained in this paper can be applied in general when determining all possible solutions of the TPBVP, which is reduced to solving a three-parameter shooting, where it is possible to estimate the interval of values of the missing parameters. Also, two procedures for realizing the brachistochronic motion of the Chaplygin sleigh are proposed.

Prior to deriving differential equations of motion the Chaplygin sleigh [10], shown in Figure 1, as well as for the needs of further considerations, two Cartesian coordinate reference systems have to be introduced. The immovable coordinate system  $Oxyz$  has a coordinate plane  $Oxy$  that coincides with the horizontal plane of motion and the movable coordinate system  $A\xi\eta\zeta$  that is stiffly attached to the knife edge, so that the coordinate plane  $A\xi\eta$  coincides with the  $Oxy$ -plane, where the  $A\xi$ -axis coincides with the orientation of the edge. Unit vectors of the movable coordinate system axes are  $\vec{\lambda}$ ,  $\vec{\mu}$  and  $\vec{\nu}$ , respectively. The configuration space for the Chaplygin sleigh is the Lie group  $SE(2)$  locally parameterized by the coordinates (generalized coordinates)  $q = (x, y, \varphi)$  on  $Q = \mathbb{R}^2 \times \mathbb{S}^1$ . Further analysis involves the case when point  $A$  is not allowed to move in the direction perpendicular to the edge, causing the occurrence of horizontal reaction of the immovable surface  $\vec{R} = R\vec{\mu}$ . Such restriction implies the nonholonomic constraints

$$\psi \equiv -\dot{x} \sin \varphi + \dot{y} \cos \varphi = 0. \quad (1)$$

AQ2



AQ3

**Figure 1.** The Chaplygin sleigh.

Such imposed constrained motion means that the velocity  $\vec{V}$  of point  $A$  of the knife edge has the direction of the axis  $A\xi$ , so the relation (1) can be expressed in the form

$$\dot{x} = V \cos \varphi, \quad \dot{y} = V \sin \varphi, \quad (2)$$

where  $V = \vec{V} \cdot \vec{\lambda}$ . As in Caratheodory [11], Neimark and Fufaev [12] and Ruina [13], we consider the case when the centre of mass of the sleigh, point  $C$ , is positioned on the  $A\xi$ -axis, that is,  $C \in A\xi$ , at the distance  $\overline{AC} = a$ . Note that in Chaplygin [10] a more general case was considered with the point  $C$  lying in the plane  $A\xi\eta$  such that  $C \notin \xi$  and  $C \notin \eta$ . The mass of the sleigh is  $m$ , whereas  $I_C$  is the moment of inertia around the principal central axis of inertia perpendicular to the  $Oxy$ -plane.

Differential equations of the sleigh motion will be created based on the general theorems of dynamics, that is, the rate of change of linear momentum as well as the rate of change of angular momentum about the centre of mass of the sleigh:

$$\frac{d\vec{K}}{dt} = \vec{F}_R^s, \quad \frac{d\vec{L}_C}{dt} = \vec{M}_C^s, \quad (3)$$

where the sleigh linear momentum is  $\vec{K} = m\vec{V}_C = m(V\vec{\lambda} + a\dot{\varphi}\vec{\mu})$ , and the sleigh angular momentum about the centre of mass is  $\vec{L}_C = I_C\dot{\varphi}\vec{v}$ . The principal force vector is  $\vec{F}_R^s = \vec{F} + \vec{R}$ , whereas the principal moment of forces about the centre of mass of the sleigh is  $\vec{M}_C^s = \overline{CA} \times \vec{R} = -aR\vec{v}$ . Observe that the control force  $\vec{F} = \vec{F}_1 + \vec{F}_2$  is acting at point  $C$ . Also, in the case of brachistochronic motion, the power of the control force equals zero,  $\vec{F} \cdot \vec{V}_C = 0$  (see e.g. Čović et al. [14]).

The following scalar differential equations correspond to vector equations (3) relative to the movable coordinate system  $A\xi\eta\zeta$ :

$$\begin{aligned} m(\dot{V} - a\dot{\varphi}^2) &= F_1, \\ m(a\ddot{\varphi} + V\dot{\varphi}) &= F_2 + R, \\ I_C\ddot{\varphi} &= -aR. \end{aligned} \quad (4)$$

The Lagrangian of the system has the following form [9]:

$$L(x_C, y_C, \varphi) = \frac{1}{2}m(\dot{x}_C^2 + \dot{y}_C^2) + \frac{1}{2}I_C\dot{\varphi}^2, \quad (5)$$

where the coordinates of the centre of mass of the sleigh are  $x_C = x + a \cos \varphi$  and  $y_C = y + a \sin \varphi$ , so after a brief rearrangement the following is obtained:

$$L(x, y, \varphi) = \frac{1}{2} m [\dot{x}^2 + \dot{y}^2 + a^2 k^2 \dot{\varphi}^2 + 2a\dot{\varphi}(-\dot{x} \sin \varphi + \dot{y} \cos \varphi)], \quad (6)$$

where  $k^2 = 1 + I_C/(ma^2)$ .

Now, differential equations of the sleigh motion will be created based on Lagrange's equations of the second kind with undetermined multipliers [15]:

$$\frac{d}{dt} \frac{\partial L}{\partial \dot{q}^\alpha} - \frac{\partial L}{\partial q^\alpha} = \tilde{Q}_\alpha + \lambda \frac{\partial \psi}{\partial \dot{q}^\alpha}, \quad \alpha = 1, 2, 3, \quad (7)$$

where  $\lambda$  is Lagrange's multiplier of the constraint, whereas  $\tilde{Q}_\alpha$  are generalized control forces. Based on (1), (6) and (7) the following is obtained:

$$\begin{aligned} m(\ddot{x} - a\ddot{\varphi} \sin \varphi - a\dot{\varphi}^2 \cos \varphi) &= F_1 \cos \varphi - F_2 \sin \varphi - \lambda \sin \varphi, \\ m(\ddot{y} + a\ddot{\varphi} \cos \varphi - a\dot{\varphi}^2 \sin \varphi) &= F_1 \sin \varphi + F_2 \cos \varphi + \lambda \cos \varphi, \\ ma[ak^2\ddot{\varphi} + \dot{\varphi}(\dot{x} \cos \varphi + \dot{y} \sin \varphi)] &= aF_2. \end{aligned} \quad (8)$$

If it is taken into account that the velocity of point  $A$  of the edge is

$$V = \dot{x} \cos \varphi + \dot{y} \sin \varphi, \quad (9)$$

after differentiation with respect to time of the constraint equation (1), and of relation (9), respectively, the following relations are obtained:

$$V\dot{\varphi} = -\dot{x} \sin \varphi + \dot{y} \cos \varphi, \quad \dot{V} = \ddot{x} \cos \varphi + \ddot{y} \sin \varphi. \quad (10)$$

Now, based on (8)–(10), the following system of equations can be formed:

$$\begin{aligned} m(\dot{V} - a\dot{\varphi}^2) &= F_1, \\ m(a\ddot{\varphi} + V\dot{\varphi}) &= F_2 + \lambda, \\ m(ak^2\ddot{\varphi} + \dot{\varphi}V) &= F_2. \end{aligned} \quad (11)$$

System (11) is equivalent to the system of equations (4), where Lagrange's multiplier of the constraint equals the reaction of a nonholonomic constraint  $\lambda = R$ .

The proposed procedure for creating differential equations of motion based on the general theorems of dynamics, as shown, is considerably simpler compared to classical procedures of forming nonholonomic systems based on the analytical mechanics [15].

The thus determined brachistochronic motion can be realized in general by the control forces, whose total power during brachistochronic motion equals zero  $\tilde{Q}_\alpha \dot{q}^\alpha = 0$ , which can be presented in the form of the active control forces, the constraint reaction forces or their mutual combinations. One of the manners of realizing the brachistochronic motion of a system, as shown, has been achieved by the active control force  $\vec{F} = \vec{F}_1 + \vec{F}_2$ , which is acting at point  $C$  (see Figure 1(a)). Note that in Antunes and Sigaud [16] the control of the Chaplygin sleigh motion is achieved by a single active force applied at point  $C$  and a single torque of active forces. Systems (4) or (11) are used as a basis for determining the laws of change of the control forces  $F_1$  and  $F_2$ , as well as the reaction of the nonholonomic constraint  $R$  as a function of defined quantities and their derivatives:

$$F_1 = m(\dot{V} - a\dot{\varphi}^2), \quad F_2 = m(ak^2\dot{\omega} + V\omega), \quad R = -\frac{I_C}{a}\dot{\omega}, \quad (12)$$

where  $\vec{\omega} = \dot{\varphi} \vec{v}$  and  $\vec{\varepsilon} = \ddot{\varphi} \vec{v}$  are the vectors of angular velocity and angular acceleration of the sleigh.

Another possible manner of realizing the brachistochronic motion of a system with two degrees of freedom (2 DOF) motion is the subsequent imposition to the system of one holonomic stationary ideal mechanical constraint (obviously, this is about the original Bernoulli's idea of realizing the control forces – the reaction force will replace the action of the active control force  $\vec{F}$ ), in accordance with previously determined brachistochronic motion, but without the action of other active forces (see Šalinić et al. [7]). The mechanical constraint has been realized by means of a smooth guide whose path-line coincides with the trajectory of point  $C$ , so that the parametric equations of the guide line are

$$\begin{aligned}x_C(t) &= x(t) + a \cos \varphi(t), \\y_C(t) &= y(t) + a \sin \varphi(t).\end{aligned}\tag{13}$$

Section 4 shows the laws of change of the control forces, as well as the trajectory of point  $C$ , at different values of the final angle of the Chaplygin sleigh in accordance with (12) and (13).

Note that in solving the system of nonlinear algebraic equations that emerged in Jeremić et al. [1] and Šalinić et al. [2,3], in the application of the shooting method, it was necessary to estimate the values of the costate variables, which is often difficult because the costate variables usually have no physical interpretations. In this regard, the most convenient is the approach from Obradović et al. [17], which does not require the estimation of the values of costate variables. However, the application of the approach from Obradović et al. [17] to a considered brachistochronic motion of the Chaplygin sleigh would require considerations of the intersection of hypersurfaces in four-dimensional (4D) space  $(x, y, \varphi, t_f)$ , where  $t_f$  is the time of the brachistochronic motion of the sleigh, which would disable us from the possibility of geometric visual representation. In this paper modification of the approach from Šalinić et al. [7] has been done by introducing two controls instead of a single one. This modification enables clear geometric estimation of the values of costate variables to be shown below.

## 2. Formulation of the brachistochrone problem and optimality conditions

Based on (2), controlled equations for the Chaplygin sleigh read

$$\dot{x} = u_1 \cos \varphi, \quad \dot{y} = u_1 \sin \varphi, \quad \dot{\varphi} = u_2,\tag{14}$$

where the control variables  $u_1(\cdot) : [t_0, t_f] \rightarrow \mathbb{R}$  and  $u_2(\cdot) : [t_0, t_f] \rightarrow \mathbb{R}$ , respectively, represent the speed  $V$  of point  $A$  and the angular velocity of the Chaplygin sleigh:

$$u_1 = V, \quad u_2 = \omega.\tag{15}$$

Such choice of control variables  $u_1$  and  $u_2$  can provide a clear physical interpretation, bearing in mind that they represent physical quantities. Also, it is possible, to be shown in Section 3, to determine the domain of definiteness of the control variables  $u_1$  and  $u_2$ . Unlike the five state equations used by Šalinić et al. [7] with a single control variable representing the angular velocity of the sleigh, introducing two control variables has enabled here to reduce the number of state equations from five to three. Let the values of the state variables and the kinetic energy of the sleigh be specified at the beginning of motion as well as the terminal boundary conditions as follows:

$$t_0 = 0, \quad x(t_0) = 0, \quad y(t_0) = 0, \quad \varphi(t_0) = 0, \quad T(t_0) = T_0,\tag{16}$$

$$t = t_f, \quad x(t_f) = x_f, \quad y(t_f) = y_f, \quad \varphi(t_f) = \varphi_f,\tag{17}$$

where  $T_0 \in \mathbb{R}$  denotes the initial kinetic energy of the sleigh and  $t_f \in \mathbb{R}$  is the final time. The sleigh is moving under the influence of control forces, their determination being not the subject of this paper (for more details on the problem of determination of these forces refer to Šalinić et al. [7]), whose power is equal to zero. Since the power of the control forces is equal to zero during the sleigh motion, the conservation of total mechanical energy of the system holds:

$$\Phi(V, \omega) \equiv V^2 + a^2 k^2 \omega^2 - \frac{2T_0}{m} = 0,\tag{18}$$

or, in accordance with incorporated control variables:

$$\Phi(u_1, u_2) \equiv u_1^2 + a^2 k^2 u_2^2 - \frac{2T_0}{m} = 0. \quad (19)$$

In order to show that the power of control forces equals zero, we will first differentiate with respect to time relation (18) where it is obtained

$$\frac{d\Phi}{dt} = V\dot{V} + a^2 k^2 \omega \dot{\omega} = 0, \quad (20)$$

whereas, on the other hand, the power of control forces  $F_1$  and  $F_2$ , taking into account (12) and (20), is determined by

$$\vec{F} \cdot \vec{V}_C = F_1 V + F_2 a \omega = m(V\dot{V} + a^2 k^2 \omega \dot{\omega}) = 0. \quad (21)$$

The brachistochronic motion problem of the Chaplygin sleigh consists in determining the controls  $u_1$  and  $u_2$  and the state variables  $x$ ,  $y$  and  $\varphi$ , so that the sleigh transfers in the minimum time  $t_f$  from the initial state (16) to the terminal state (17). This can be expressed as the minimization of the following action functional:

$$J(q, u) = \int_{t_0}^{t_f} dt, \quad (22)$$

where  $u = (u_1, u_2)$ , subject to (14), (16), (17), and the control constraint (19), where  $t_f$  is free.

To solve the optimal control problem formulated by Pontryagin's maximum principle [18], the augmented (extended) Hamiltonian [19] is formed as

$$H(q, u, \lambda) = \lambda_0 + \lambda_x u_1 \cos \varphi + \lambda_y u_1 \sin \varphi + \lambda_\varphi u_2 + \mu \Phi(u_1, u_2), \quad (23)$$

where the sum of the first four terms in (23) represents the Hamilton–Pontryagin Hamiltonian [18],  $\lambda_0 = \text{const.} \leq 0$ ,  $\lambda_x(\cdot) : [t_0, t_f] \rightarrow \mathbb{R}$ ,  $\lambda_y(\cdot) : [t_0, t_f] \rightarrow \mathbb{R}$  and  $\lambda_\varphi(\cdot) : [t_0, t_f] \rightarrow \mathbb{R}$  are the costate variables associated with  $x$ ,  $y$  and  $\varphi$ , respectively, and  $\mu(\cdot) : [t_0, t_f] \rightarrow \mathbb{R}$  is the Lagrange multiplier. Hence, the corresponding costate equations [18, 19] read

$$\dot{\lambda}_x = -\frac{\partial H}{\partial x} = 0, \quad \dot{\lambda}_y = -\frac{\partial H}{\partial y} = 0, \quad \dot{\lambda}_\varphi = -\frac{\partial H}{\partial \varphi} = (\lambda_x \sin \varphi - \lambda_y \cos \varphi) u_1, \quad (24)$$

with the transversality condition  $H(t_f) = 0$  associated with the final time  $t_f$ .

The Legendre necessary conditions of optimality of the Hamiltonian  $H$  with respect to the controls  $u_1$  and  $u_2$  read [19]

$$\left( \frac{\partial H}{\partial u_i} \right)_{u^{opt}} = 0, \quad \left( \frac{\partial^2 H}{\partial u_i \partial u_j} \right)_{u^{opt}} u_i u_j \leq 0, \quad (i, 2j = 1, 2). \quad (25)$$

Since the Hamiltonian has no explicit time dependence, then a first integral of the motion is  $H(t) = \text{const.}$ , or, taking into account (19) and  $H(t_f) = 0$ :

$$\lambda_0 + \lambda_x u_1 \cos \varphi + \lambda_y u_1 \sin \varphi + \lambda_\varphi u_2 + \mu \Phi(u_1, u_2) = 0. \quad (26)$$

From (24)<sub>1,2</sub> it follows that  $\lambda_x = \text{const.}$ ,  $\lambda_y = \text{const.}$  for  $t \in [t_0, t_f]$ . Now, based on (25)<sub>1</sub>, it is obtained that

$$\lambda_x \cos \varphi + \lambda_y \sin \varphi = -2\mu u_1, \quad \lambda_\varphi = -2\mu a^2 k^2 u_2, \quad (27)$$

while from (19) it follows that

$$u_1^2 + a^2 k^2 u_2^2 = \frac{2T_0}{m}. \quad (28)$$

Introducing (27) and (28) into (26) yields the expression for the multiplier  $\mu$ :

$$\mu = \frac{\lambda_0 m}{4T_0}. \quad (29)$$

Now, if one takes  $\lambda_0 = 0$  one has an abnormal brachistochrone problem [19]. Let us show that the considered brachistochrone problem is not abnormal. If  $\lambda_0 = 0$  then from (27) and (29) it follows that  $\mu(t) \equiv 0$ ,  $\lambda_\varphi(t) \equiv 0$ ,  $\lambda_x \equiv 0$  and  $\lambda_y \equiv 0$ , that is, all costate variables are identically equal to zero. Consequently, the necessary conditions of Pontryagin's maximum principle [18] are not satisfied using  $\lambda_0 = 0$ , since all costate variables cannot be identically zero. Next, the normal brachistochrone problem is considered where, according to Pontryagin et al. [18], it can be taken that  $\lambda_0 = -1$ . Now, based on (25)<sub>1</sub> and (29), the expressions for the control variables can be written as

$$u_1 = \frac{2T_0}{m} (\lambda_x \cos \varphi + \lambda_y \sin \varphi), \quad u_2 = \frac{2T_0}{m} \frac{1}{a^2 k^2} \lambda_\varphi. \quad (30)$$

Finally, introducing the initial conditions (16) and the relations (29) and (30) into (26) gives

$$\lambda_\varphi(t_0) = \pm ak \sqrt{\frac{m}{2T_0} - \lambda_x^2}. \quad (31)$$

### 3. Formulation of a two-point boundary-value problem

In accordance to the above relations, the TPBVP corresponding to the brachistochrone problem considered is determined by the following differential equations:

$$\begin{aligned} \dot{x} &= \frac{2T_0}{m} (\lambda_x \cos \varphi + \lambda_y \sin \varphi) \cos \varphi, \\ \dot{y} &= \frac{2T_0}{m} (\lambda_x \cos \varphi + \lambda_y \sin \varphi) \sin \varphi, \end{aligned} \quad (32)$$

$$\begin{aligned} \dot{\varphi} &= \frac{2T_0}{m} \frac{1}{a^2 k^2} \lambda_\varphi, \\ \dot{\lambda}_\varphi &= \frac{2T_0}{m} (\lambda_x \cos \varphi + \lambda_y \sin \varphi) (\lambda_x \sin \varphi - \lambda_y \cos \varphi), \end{aligned} \quad (33)$$

with the initial boundary conditions

$$t_0 = 0, \quad x(t_0) = 0, \quad y(t_0) = 0, \quad \varphi(t_0) = 0, \quad \lambda_\varphi(t_0) = \pm ak \sqrt{\frac{m}{2T_0} - \lambda_x^2}. \quad (34)$$

Now, based on (12), (30) and (33) one can determine the laws of change of the control forces  $F_1$  and  $F_2$  as well as the reactions of nonholonomic constraint  $R$ :

$$\begin{aligned} F_1 &= - \left( \frac{2T_0}{m^{1/2} ak} \right)^2 \left( \lambda_x \sin \varphi - \lambda_y \cos \varphi + \frac{1}{ak^2} \lambda_\varphi \right) \lambda_\varphi, \\ F_2 &= \frac{4T_0^2}{ma} (\lambda_x \cos \varphi + \lambda_y \sin \varphi) \left( \lambda_x \sin \varphi - \lambda_y \cos \varphi + \frac{1}{ak^2} \lambda_\varphi \right), \\ R &= - \frac{I_C}{a} \left( \frac{2T_0}{mak} \right)^2 (\lambda_x \cos \varphi + \lambda_y \sin \varphi) (\lambda_x \sin \varphi - \lambda_y \cos \varphi). \end{aligned} \quad (35)$$



The numerical procedure for solving this TPBVP is based on the shooting method [4]. Namely, solving the corresponding Cauchy's problem (32) and (33) with the conditions (34), the following relations can be established in a numerical form:

$$x_f = f_x(\lambda_x, \lambda_y, t_f), \quad y_f = f_y(\lambda_x, \lambda_y, t_f), \quad \varphi_f = f_\varphi(\lambda_x, \lambda_y, t_f). \quad (36)$$

Each of the relations (36) can be graphically represented by a surface in  $\mathbb{R}^3$  with axes  $\lambda_x, \lambda_y$  and  $t_f$  and the intersection of these surfaces represents the solution of the system of equations (36). In the case of several crossing points (several solutions of the TPBVP) occurring in the part of the space corresponding to allowable values of the quantities and  $\lambda_x, \lambda_y$  and  $t_f$ , the global minimum time at the brachistochronic motion of the Chaplygin sleigh corresponds to the crossing point with the minimum time  $t_f$ . When solving the TPBVP in the thus described manner, a need is naturally imposed to estimate the interval within which the values of quantities  $\lambda_x$  and  $\lambda_y$  range. For the considered problem, this estimation is easy to perform. Namely, from the condition that the expression under the radical in (31) must be nonnegative (zero or positive), there follows the estimation of the interval of values of the quantity  $\lambda_x$ :

$$-\sqrt{\frac{m}{2T_0}} \leq \lambda_x \leq \sqrt{\frac{m}{2T_0}}. \quad (37)$$

Based on the quadratic form of control (19), one can determine the domain of definiteness of the controls  $u_1$  and  $u_2$ :

$$-\sqrt{\frac{2T_0}{m}} \leq u_1 \leq \sqrt{\frac{2T_0}{m}}, \quad -\sqrt{\frac{2T_0}{ma^2k^2}} \leq u_2 \leq \sqrt{\frac{2T_0}{ma^2k^2}}. \quad (38)$$

Now, based on (30) and (38), the following dual inequality can be derived:

$$-\sqrt{\frac{m}{2T_0}} \leq \lambda_x \cos \varphi_f + \lambda_y \sin \varphi_f \leq \sqrt{\frac{m}{2T_0}}. \quad (39)$$

Taking into account (37) and (39) one can perform estimation of the interval of values of the quantity  $\lambda_y$ , which is necessary to provide in applying the shooting method, depending on the final angle of the edge  $\varphi_f$ :

$$-\sqrt{\frac{m}{2T_0}} \cot \frac{\varphi_f}{2} \leq \lambda_y \leq \sqrt{\frac{m}{2T_0}} \cot \frac{\varphi_f}{2}, \quad \forall \varphi_f \neq 0. \quad (40)$$

Note that at the final angle value of the edge  $\varphi_f = 0$ , as well as at the value  $\varphi_f = \pi$ , the estimation of the interval of values of the quantity  $\lambda_y$  cannot be provided, and therefore these cases will be separately considered in the next section.

Now, taking into account the estimation of the interval of values (37) and (40), where  $t_f \geq 0$ , it can be asserted that all solutions of the corresponding TPBVP fall within the defined interval of values.

Based on the above considerations, it is possible now to determine the intersections of the surfaces (36) as

$$p_f = f_x(\lambda_x, \lambda_y, t_f) \cap f_y(\lambda_x, \lambda_y, t_f), \quad q_f = f_x(\lambda_x, \lambda_y, t_f) \cap f_\varphi(\lambda_x, \lambda_y, t_f), \quad (41)$$

where  $p_f$  and  $q_f$  are space curves represented by the following dependencies in the numerical form:

$$p_f = f_p(\lambda_x, t_f), \quad q_f = f_q(\lambda_x, t_f). \quad (42)$$

Now, the solutions of the TPBVP can be represented by the geometric crossing points of curves (42) as

$$f_p(\lambda_x, t_f) \cap f_q(\lambda_x, t_f) = M_1, M_2, \dots, M_n. \quad (43)$$

The number of elements of the set (43) is equal to the number of all possible solutions of the TPBVP.

From the viewpoint of how easy it is to observe the crossing points  $M_i$  and to visually estimate their coordinates, the described method is better to use than the surface crossing method (used by Jeremić et al. [1]). In the next section we will see how a comparative presentation of both methods is given.

Now, it is possible by applying the surface crossing method (36) or the space curves crossing method (42) to perform the estimation of the values of coordinates  $(\lambda_x^*, \lambda_y^*, t_f^*)$  of all crossing points (43). The estimated values of coordinates  $(\lambda_x^*, \lambda_y^*, t_f^*)$  of the crossing points can be used as initial iteration for finding accurate values of the quantities  $\lambda_x, \lambda_y$  and  $t_f$  by applying the shooting method, whose detailed description is presented in the Appendix.

In the work, the implementation of the crossing of curves (42) is achieved by using the built-in ContourPlot3D() Mathematica function (see e.g. Ruskeepää [20]).

## 4. Numerical examples

In this section, the TPBVP formulated in Section 3 is solved for the following values of the sleigh parameters:  $m = 2\text{kg}$ ,  $a = 1\text{m}$ ,  $x_f = 1\text{m}$ ,  $y_f = 1\text{m}$ ,  $k = 1.5$ ,  $T_0 = 200 \frac{\text{kg m}^2}{\text{s}^2}$ , and the influence of the final position of  $\varphi$ ,  $\varphi_f$  on the appearance of multiple extremals in the Chaplygin sleigh brachistochrone problem is examined.

### 4.1. The case of the value $\varphi_f = \pi/2$

In order to compare the results obtained in the present paper with the results obtained by Šalinić et al. [7] and to show that the obtained solution is optimal, we will first consider the case when  $\varphi_f = \pi/2$ .

Based on (37) and (40), the following estimations can be made:

$$-0.0707 \leq \lambda_x \leq 0.0707, \quad -0.0707 \leq \lambda_y \leq 0.0707. \quad (44)$$

From Figures 2 and 3, taking into account that the corresponding surfaces and space curves, respectively, are crossing only at one point, it can be claimed with certainty that there is a solution of the TPBVP for the case  $\varphi_f = \pi/2$ , as well as that it is optimal. Figure 2(a) shows the crossing of surfaces (36) in the interval  $0 \leq t_f \leq 0.6$ , while Figure 2(b) shows the crossing of surfaces for a narrower interval, so as to make the crossing point of surfaces more visible. Figure 3 shows the crossing of space curves  $p$  and  $q$ , where crossing point  $M$  is clearly visible, whose coordinates in three-dimensional (3D) space  $(\lambda_x, \lambda_y, t_f)$  correspond to the TPBVP solution. Visual estimation of the values of coordinates of the

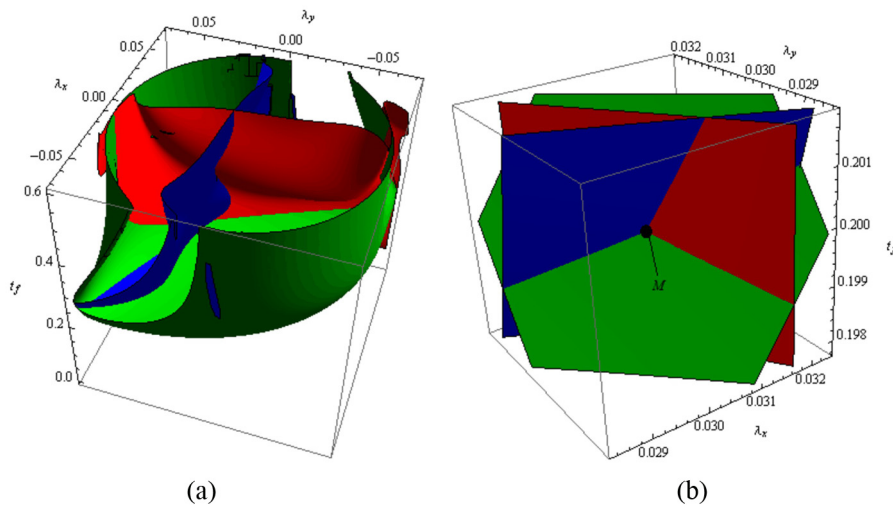


**Figure 2.** Crossing of surfaces  $x_f = f_x(\lambda_x, \lambda_y, t_f)$ ,  $y_f = f_y(\lambda_x, \lambda_y, t_f)$  and  $\varphi_f = f_\varphi(\lambda_x, \lambda_y, t_f)$  for  $\varphi_f = \pi/2$ .

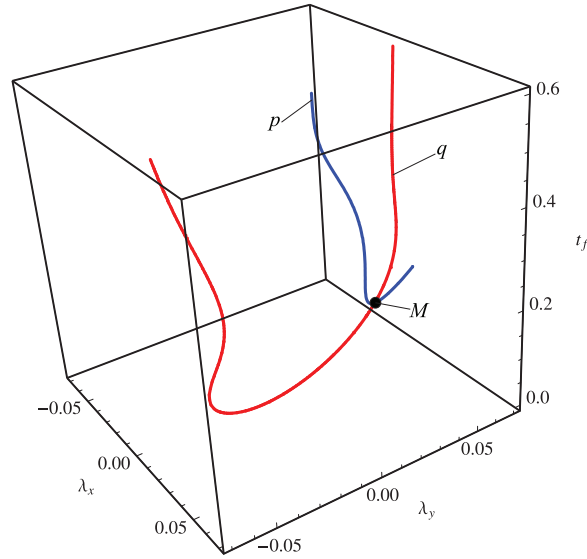


**Figure 3.** Crossing of curves  $p_f = f_p(\lambda_x, t_f)$  and  $q_f = f_q(\lambda_x, t_f)$  for  $\varphi_f = \pi/2$ .

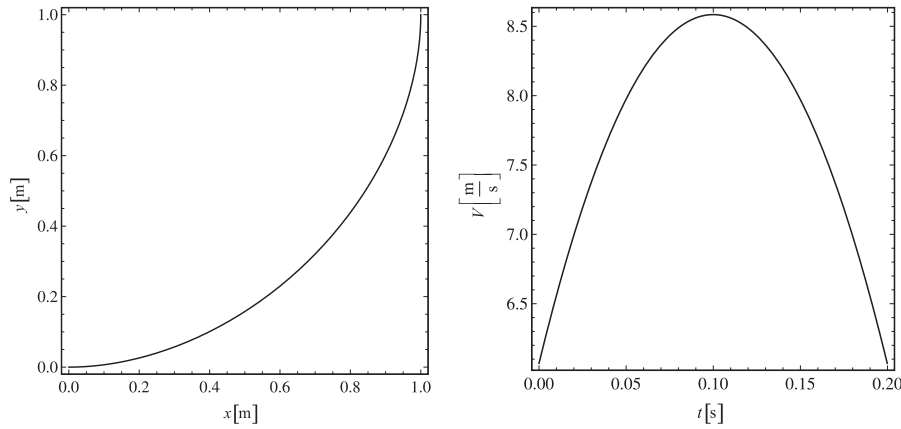


**Figure 4.** The trajectory of point A and graph of speed  $V$  for  $\varphi_f = \pi/2$ .

crossing point  $M$  from Figure 3 are  $(0, 0, 0.2)$ , which represent the initial iteration for finding accurate values by applying the shooting method.

Applying the procedure from Section 3 it is obtained that  $t_f = 0.199832$  s,  $\lambda_x = 0.0303507$ s/m and  $\lambda_y = 0.0303507$ s/m. This result coincides with the one obtained by Šalinić et al. [7].

The trajectory of point  $A$  as well as the graph of speed  $V$  is shown in Figure 4.

The laws of change of the control forces  $F_1$  and  $F_2$ , based on (35), for realizing the Chaplygin sleigh brachistochronic motion are shown in Figure 5.

The law of change of the reaction of nonholonomic constraint  $R$  and the trajectory of point  $C$  are shown in Figure 6. In Figure 6 point  $C_0$  represents the initial, whereas point  $C_f$  represents the final position of point  $C$  of the edge.

#### 4.2. The case of the value $\varphi_f = \pi/30$

Taking into account that we cannot make estimation of the value of quantity  $\lambda_y$  when the final angle value of the edge is  $\varphi_f = 0$ , we will first perform estimation, as well as the solutions of the corresponding TPBVP, at a close value of the final angle of the edge  $\varphi_f = \pi/30$ .

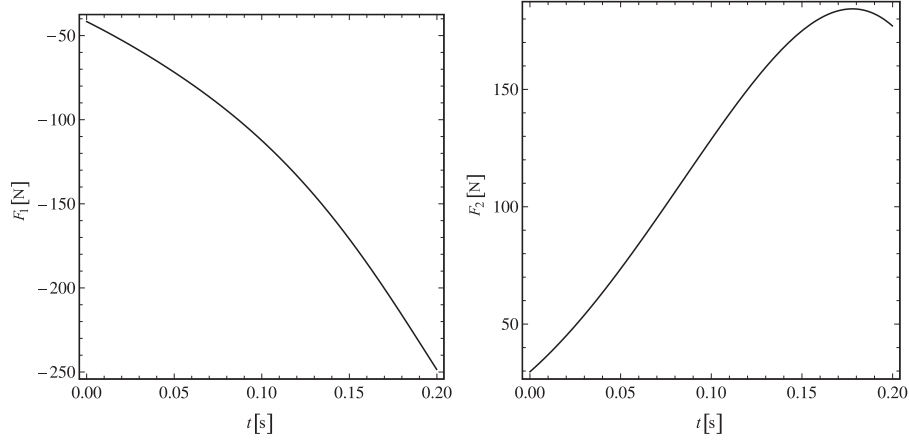


**Figure 5.** Control forces  $F_1$  and  $F_2$  for  $\varphi_f = \pi/2$ .

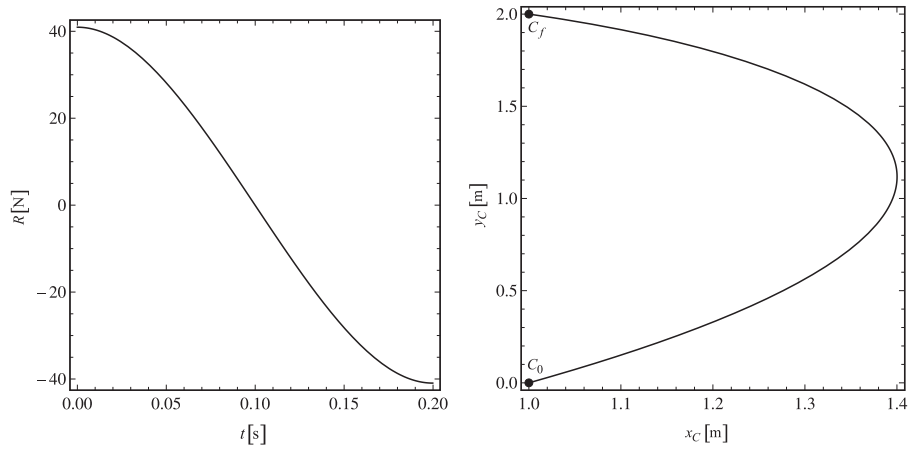


**Figure 6.** Reaction of the nonholonomic constraint  $R$  and trajectory of point  $C$  for  $\varphi_f = \pi/2$ .

In this case, from (37) and (39) it follows that

$$-0.0707 \leq \lambda_x \leq 0.0707, \quad -(0.6765 + 9.5144\lambda_x) \leq \lambda_y \leq 0.6765 - 9.5144\lambda_x, \quad (45)$$

respectively, based on (40) it is

$$-1.3492 \leq \lambda_y \leq 1.3492. \quad (46)$$

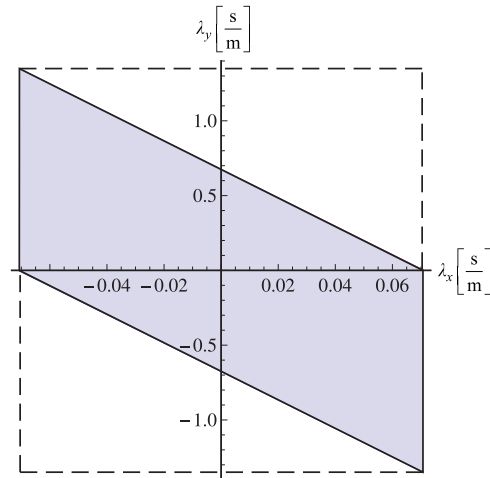
Graphical representation of the estimations (45) is given in Figure 7.

The shaded region in Figure 7 corresponds to the estimations given by (45).

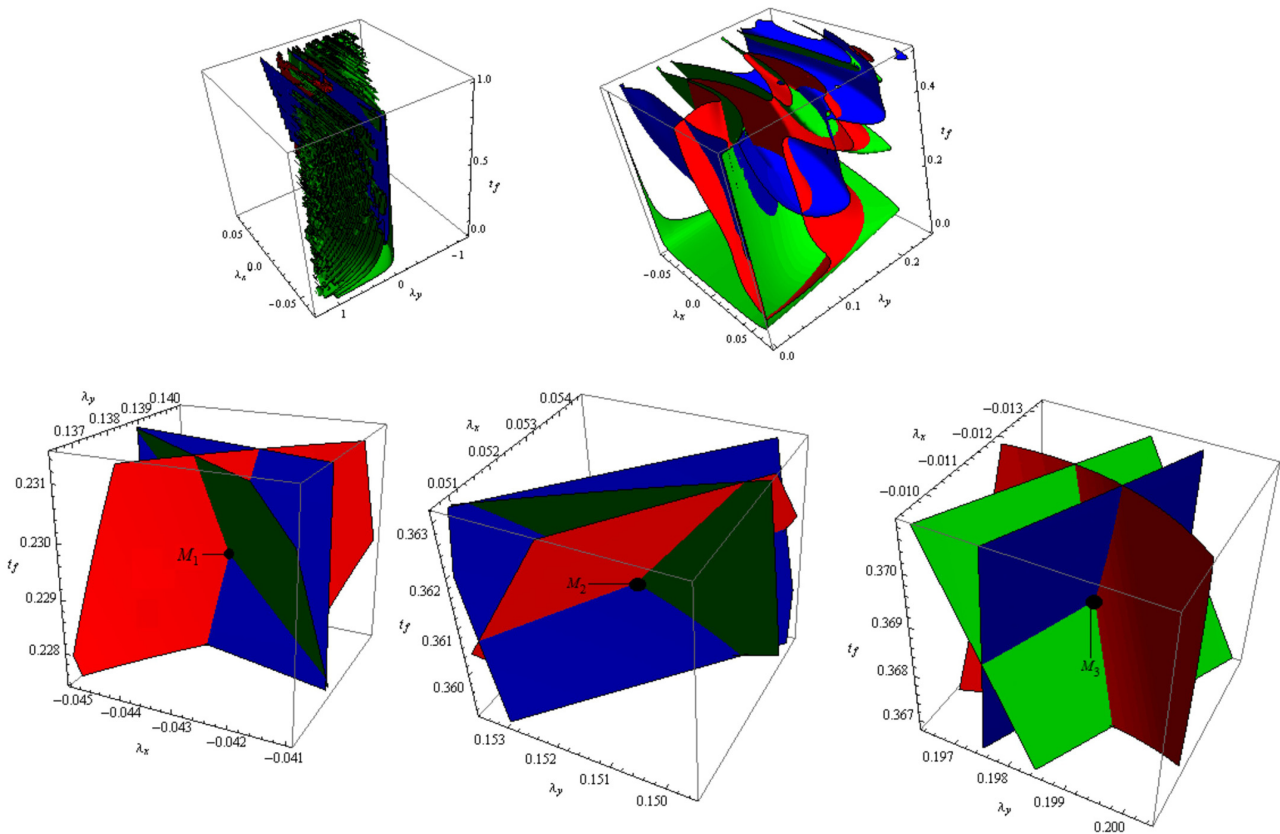
In Figures 8 and 9 the crossing of surfaces (36) and the crossing of curves (42), respectively, are shown. We can observe from Figures 8 and 9 that the solution of the TPBVP is not unique. To find all possible solutions of the TPBVP, it is more convenient to use a graphic analysis of the solution in 3D space of the missing parameters, as shown in Figures 8 and 9.

Visual estimation of the values of coordinates of the crossing points  $M_1, M_2$  and  $M_3$ , respectively, from Figure 9 are  $(0, 0.1, 0.2)$ ,  $(0, 0.15, 0.4)$  and  $(0, 0.2, 0.4)$ .

All solutions of the TPBVP in the interval  $0 \leq t_f \leq 0.6$ , shown in Table 1, which are represented by the crossing points  $M_1, M_2$  and  $M_3$  of the space curves  $p$  and  $q$ , are given in Figure 9. The trajectories and velocities of point  $A$  corresponding to the crossing points  $M_1, M_2$  and  $M_3$  are shown in Figure 10. In



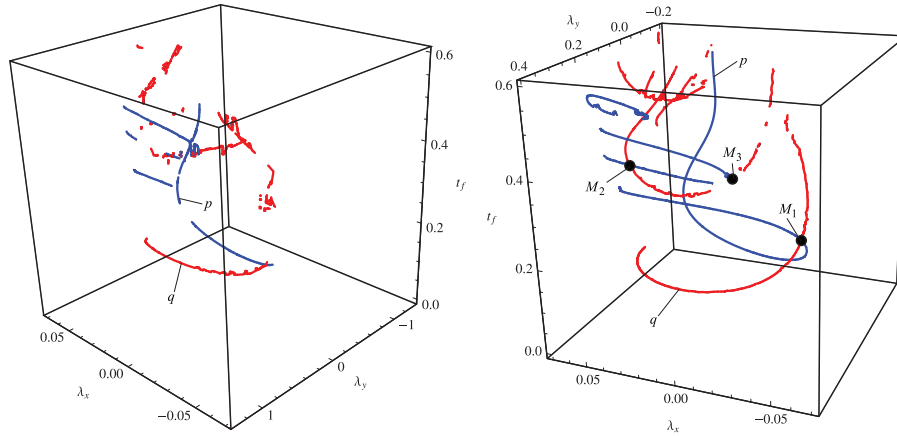
**Figure 7.** Estimation of the quantities  $\lambda_x$  and  $\lambda_y$  for  $\varphi_f = \pi/30$ .



**Figure 8.** Cross-section of surfaces  $x_f = f_x(\lambda_x, \lambda_y, t_f)$ ,  $y_f = f_y(\lambda_x, \lambda_y, t_f)$  and  $\varphi_f = f_\varphi(\lambda_x, \lambda_y, t_f)$  at  $\varphi_f = \pi/30$ .

Figure 10,  $A_0$  represents the initial and  $A_f$  the final position of point  $A$ . Based on the values shown in Table 1, it can be concluded that the global minimum time is achieved in the case of the first solution (point  $M_1$  shown in Figures 8 and 9) and it equals  $t_f = 0.229455$  s.

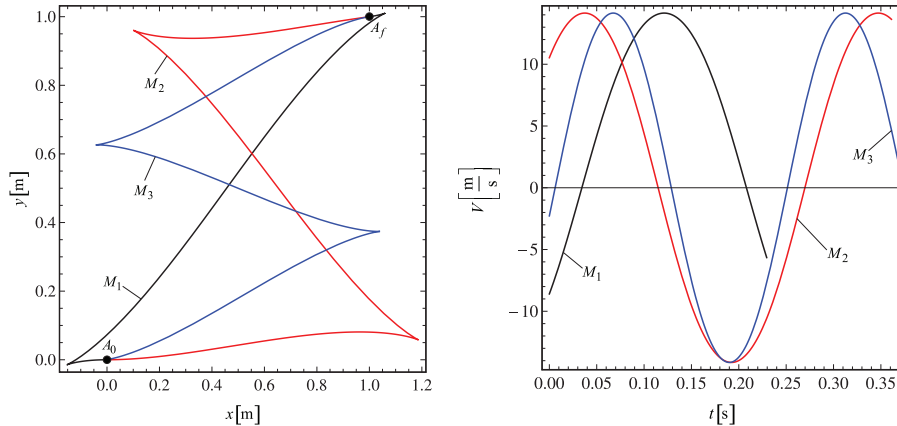
Two stopping points correspond to the solutions  $M_1$  and  $M_2$ , whereas three stopping points correspond to the solution  $M_3$ , that is, the positions where the velocity of the contact point between the knife edge and the horizontal plane equals zero.



**Figure 9.** Crossing of curves  $p_f = f_p(\lambda_x, t_f)$  and  $q_f = f_q(\lambda_x, t_f)$  for  $\varphi_f = \pi/30$ .

**Table I.** The two-point boundary-value problem solutions for the case of the value  $\varphi_f = \pi/30$ .

Solutions	$\lambda_x [2s/m]$	$\lambda_y [2s/m]$	$t_f [2s]$
First solution ( $M_1$ )	-0.042973	0.138484	0.229455
Second solution ( $M_2$ )	0.0526389	0.151529	0.361141
Third solution ( $M_3$ )	-0.0113855	0.198418	0.368861



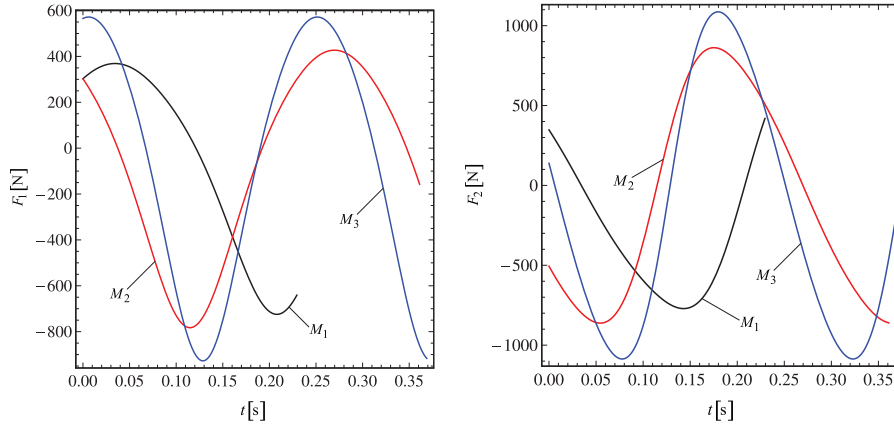
**Figure 10.** The trajectories and speeds of point A for  $\varphi_f = \pi/30$  corresponding to the solutions shown in Table I.

Figure 11 shows the laws of change of the control forces  $F_1$  and  $F_2$  corresponding to the solutions given in Table I.

Figure 12 shows the law of change of the reaction of nonholonomic constraint  $R$  and the trajectories of point C corresponding to the solutions presented in Table I.

#### 4.3. The case of the value $\varphi_f = 0$

For the value of the angle  $\varphi_f = 0$ , based on (40), only the value of the quantity  $\lambda_x$ , highlighted in Section 4.2, can be estimated. Due to the closeness of values  $\varphi_f = 0$  and  $\varphi_f = \pi/30$ , the estimation for  $\lambda_y$  from Section 4.2 was used.



**Figure 11.** Control forces  $F_1$  and  $F_2$  for  $\varphi_f = \pi/30$  corresponding to the solutions shown in Table 1.

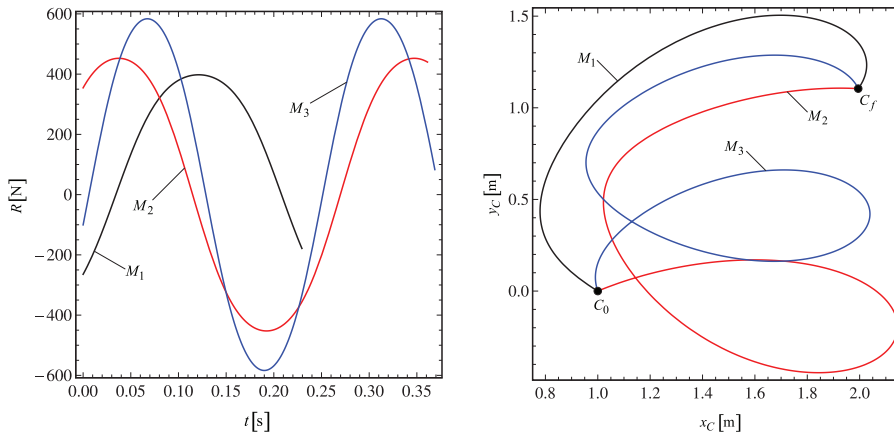


**Figure 12.** Reactions of the nonholonomic constraint  $R$  and trajectories of point  $C$  for  $\varphi_f = \pi/30$  corresponding to the solutions shown in Table 1.

In Figures 13 and 14, respectively, the crossing of surfaces (36) and the crossing of curves (42) are shown. We can observe from Figures 13 and 14 that the TPBVP solution is not unique. Visual estimation of the values of coordinates of the crossing points  $M_1, M_2$  and  $M_3$ , respectively, from Figure 14 are  $(0, 0.15, 0.2)$ ,  $(0, 0.15, 0.4)$  and  $(0, 0.2, 0.4)$ .

Based on Figures 13 and 14, all the TPBVP solutions in the interval  $0 \leq t_f \leq 0.6$  are shown in Table 2. The trajectory and velocity of point  $A$ , respectively, corresponding to the crossing points  $M_1, M_2$  and  $M_3$  are presented in Figure 15. The global minimum time in the brachistochronic motion of the sleigh corresponding to the terminal value  $\varphi_f = 0$  is determined by the first solution (point  $M_1$  shown in Figures 13 and 14) and it equals  $t_f = 0.239187s$ .

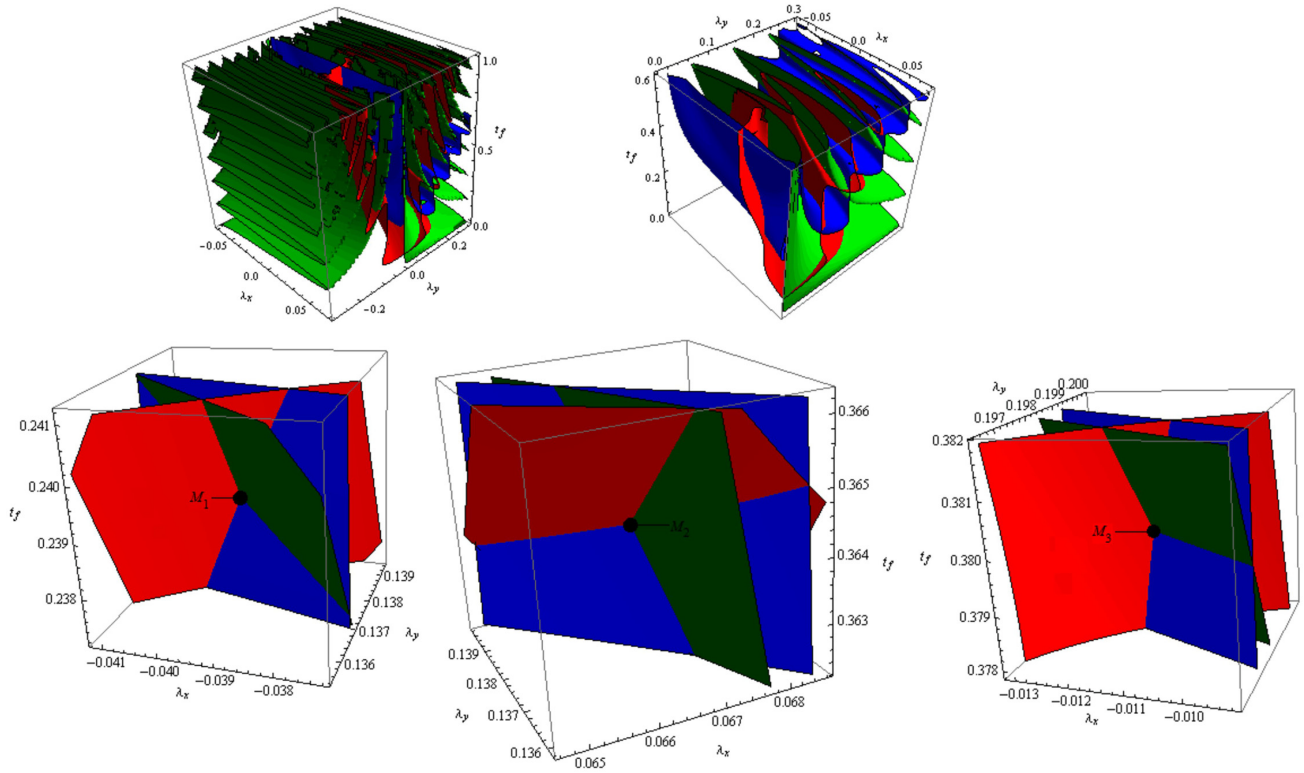
Two stopping points correspond to the solutions  $M_1$  and  $M_2$ , whereas four stopping points correspond to the solution  $M_3$ .

Figure 16 shows the laws of change of the control forces  $F_1$  and  $F_2$  corresponding to the solutions presented in Table 2.

Figure 17 shows the laws of change of the reactions of nonholonomic constraint  $R$  and the trajectories of point  $C$  corresponding to the solutions presented in Table 1.

#### 4.4. The case of the value $\varphi_f = \pi$

As mentioned above, at the final angle value of the edge  $\varphi_f = \pi$ , the estimation of the interval of values of the quantity  $\lambda_y$  cannot be made. In this case, estimation will be deployed for the interval of values of



**Figure 13.** Crossing of surfaces  $x_f = f_x(\lambda_x, \lambda_y, t_f)$ ,  $y_f = f_y(\lambda_x, \lambda_y, t_f)$  and  $\varphi_f = f_\varphi(\lambda_x, \lambda_y, t_f)$  for  $\varphi_f = 0$ .

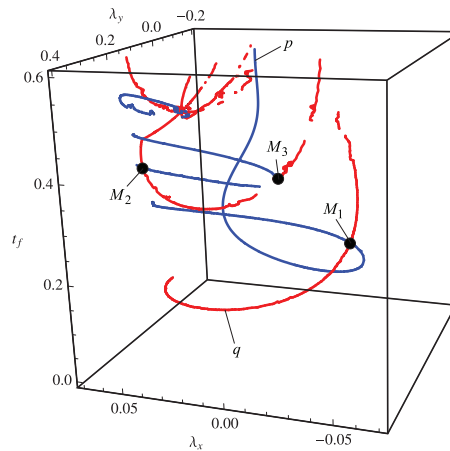


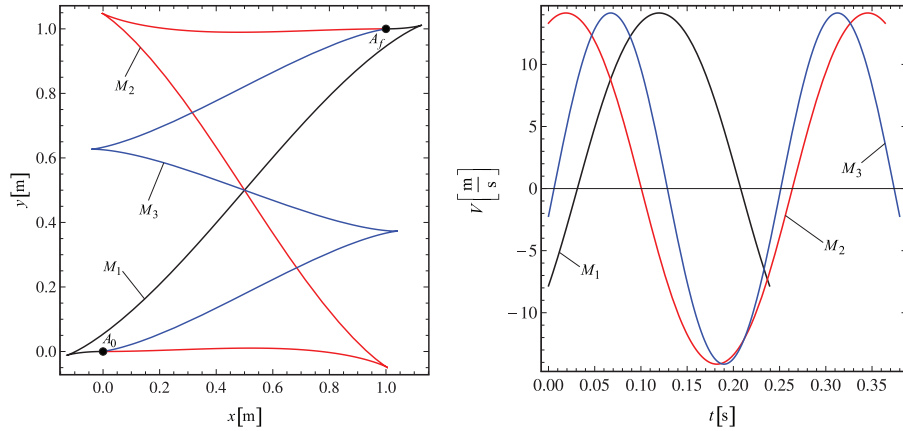
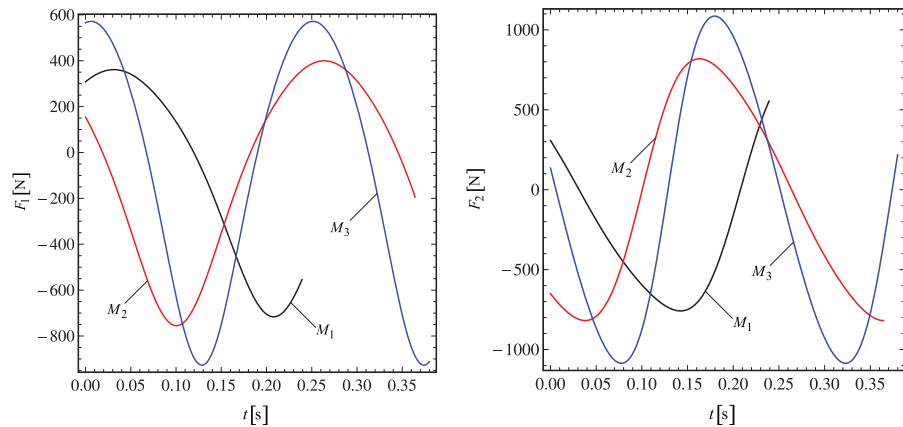
**Figure 14.** Crossing of curves  $p_f = f_p(\lambda_x, t_f)$  and  $q_f = f_q(\lambda_x, t_f)$  for  $\varphi_f = 0$ .

the quantities  $\lambda_x, \lambda_y$  given in (44). From Figures 18 and 19, taking into account that the corresponding surfaces and space curves, respectively, are crossing only at one point, it can be asserted that the obtained solution of the TPVBP for the case  $\varphi_f = \pi$  is optimal. Visual estimation of the values of coordinates of the crossing point  $M$  from Figure 19 are  $(0, 0, 0.3)$ , which represent the initial iteration for finding the accurate values by applying the shooting method. The solutions of the TPBVP for the case  $\varphi_f = \pi$  in the interval  $0 \leq t_f \leq 0.6$  are  $t_f = 0.199832$  s,  $\lambda_x = 0.0303507$  s/m and  $\lambda_y = 0.0303507$  s/m. The trajectory of point  $A$ , as well as the graph of speed  $V$ , is shown in Figure 20.



**Table 2.** The two-point boundary-value problem solutions for the case of the value  $\varphi_f = 0$ .

Solutions	$\lambda_x [2s/m]$	$\lambda_y [2s/m]$	$t_f [2s]$
First solution ( $M_1$ )	-0.0391831	0.137402	0.239187
Second solution ( $M_2$ )	0.0666096	0.137803	0.364262
Third solution ( $M_3$ )	-0.0111406	0.198342	0.379927

**Figure 15.** The trajectory and speed of point A for  $\varphi_f = 0$  corresponding to the solutions shown in Table 2.**Figure 16.** Control forces  $F_1$  and  $F_2$  for  $\varphi_f = 0$  corresponding to the solutions shown in Table 2.

One position corresponds to the case  $\varphi_f = \pi$ , where the velocity of the contact point between the knife edge and the horizontal plane equals zero.

The laws of change of the control forces  $F_1$  and  $F_2$  for realizing the Chaplygin sleigh brachistochronic motion for the final angle value  $\varphi_f = \pi$  are shown in Figure 21.

The law of change of the reaction of nonholonomic constraint  $R$  as well as the trajectories of point C for the final angle value  $\varphi_f = \pi$  are shown in Figure 22.

## 5. Conclusions

This paper presents a new procedure for the determination of the global minimum time in the brachistochronic motion of the Chaplygin sleigh. The new procedure is based on previous estimation of the

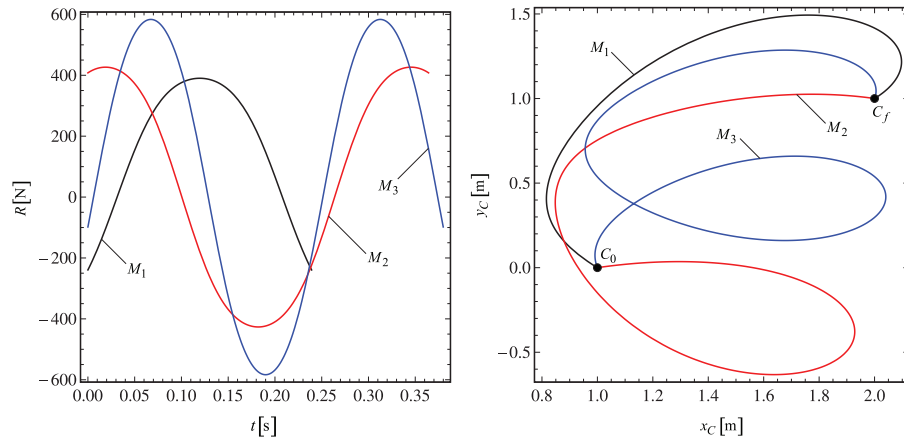


**Figure 17.** Reactions of the nonholonomic constraint  $R$  and trajectories of point  $C$  for  $\varphi_f = 0$  corresponding to the solutions shown in Table 2.

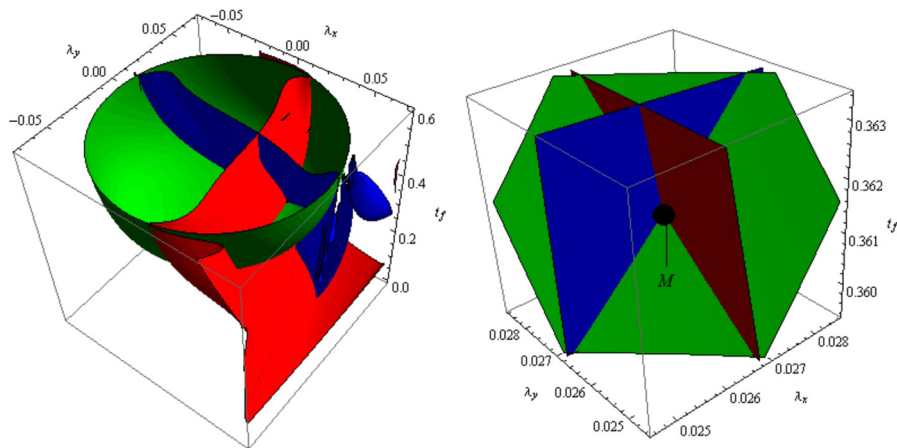


**Figure 18.** Crossing of surfaces  $x_f = f_x(\lambda_x, \lambda_y, t_f)$ ,  $y_f = f_y(\lambda_x, \lambda_y, t_f)$  and  $\varphi_f = f_\varphi(\lambda_x, \lambda_y, t_f)$  for  $\varphi_f = \pi$ .

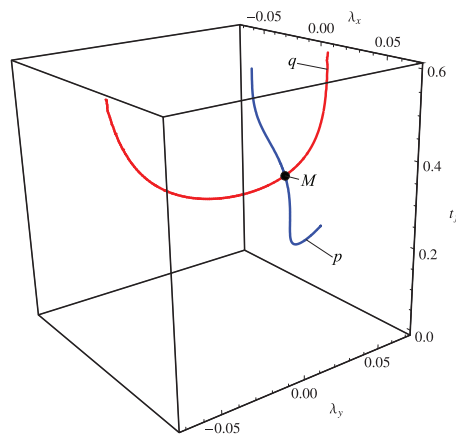


**Figure 19.** Crossing of curves  $p_f = f_p(\lambda_x, t_f)$  and  $q_f = f_q(\lambda_x, t_f)$  for  $\varphi_f = \pi$ .

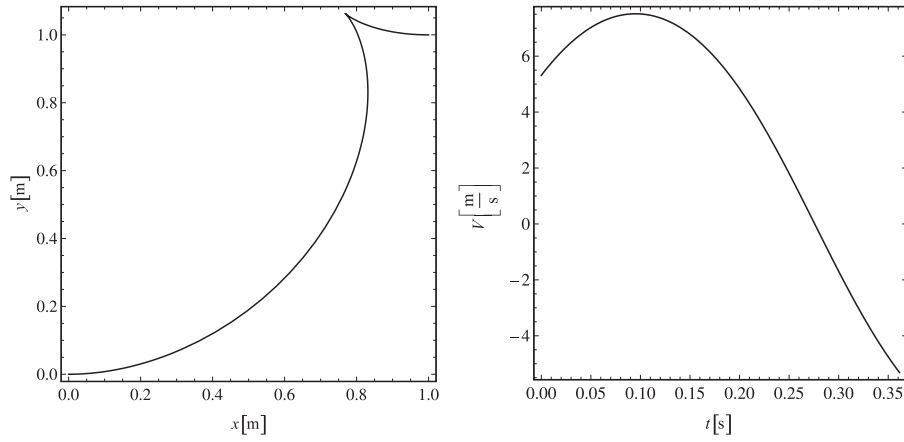


**Figure 20.** The trajectory of point A and graph of speed  $V$  for  $\varphi_f = \pi$ .

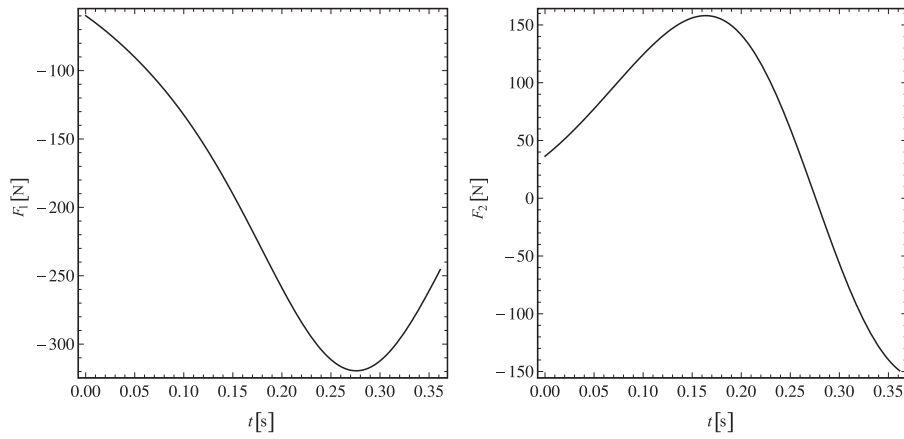


**Figure 21.** Control forces  $F_1$  and  $F_2$  for  $\varphi_f = \pi$ .

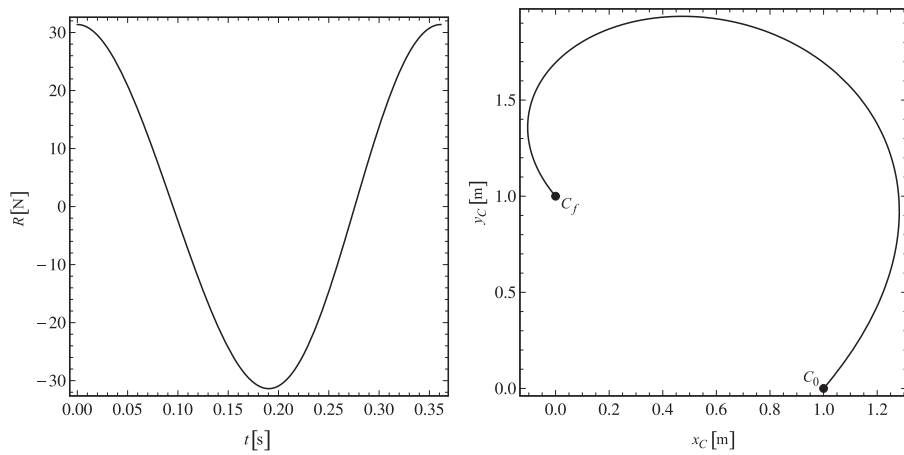


**Figure 22.** Reaction of the nonholonomic constraint  $R$  and trajectory of point C for  $\varphi_f = \pi$ .

interval of values of the unknown quantities  $\lambda_x$  and  $\lambda_y$ , where  $t_f \geq 0$ , so that all solutions of the corresponding TPBVP fall within the defined interval of values. For the case of multiple solutions of the TPBVP, the global minimum time is that solution which corresponds to the minimum time.

Since the TPBVP is reduced to the solving of three-parameter shooting, all solutions of the TPBVP can be graphically represented in  $\mathbb{R}^3$  with axis  $\lambda_x$ ,  $\lambda_y$  and  $t_f$  as an intersection of corresponding space curves (42). In that case, the number of crossing points equals the number of all possible solutions, whereas the coordinates of the crossing points represent the solutions of the TPBVP.

This method is more convenient than the method of the crossing of surfaces (36) because the method of the crossing of surfaces often causes difficulties, which refers to the clear observation of the number of crossing points and their coordinates. Unlike the case of  $\varphi_f = \pi/2$  considered by Šalinić et al. [7], for  $\varphi_f \neq \pi/2$  during the brachistochronic motion of the sleigh there are sleigh positions, where the velocity of the contact point of the knife edge with the horizontal plane equals zero. Exactly this position corresponds to the instant stopping position of point  $A$  of the edge, that is, the position where point  $A$  changes the direction of motion. Also, two modes are presented for the realization of the Chaplygin sleigh brachistochronic motion, where the laws of change of the control forces are determined too and guide path-lines for different values of the edge final angle.

## Funding

This research received no specific grant from any funding agency in the public, commercial or not-for-profit sectors.

**AQ7**

## References

- [1] Jeremić, O, Šalinić, S, Obradović, A, et al. On the brachistochrone of a variable mass particle in general force fields. *Math Comput Model* 2011; 54: 2900-2912.
- [2] Šalinić, S, Obradović, A, Mitrović, Z, et al. Brachistochrone with limited reaction of constraint in an arbitrary force field. *Nonlinear Dynam* 2012; 69: 211-222.
- [3] Šalinić, S, Obradović, A, Mitrović, Z, et al. Erratum to: Brachistochrone with limited reaction of constraint in an arbitrary force field. *Nonlinear Dynam* 2012; 70: 891-892.
- [4] Stoer, J, and Bulirsch, J. *Introduction to numerical analysis*. Berlin: Springer, 1993.
- [5] Obradović, A, Čović, V, Vesković, M, et al. Brachistochronic motion of a nonholonomic mechanical system. *Acta Mech* 2010; 214: 291-304.
- [6] Radulović, R, Zeković, D, Lazarević, M, et al. Analysis the brachistochronic motion of a mechanical system with non-linear nonholonomic constraint. *FME Trans* 2014; 42: 290-296.
- [7] Šalinić, S, Obradović, A, Mitrović, Z, et al. On the brachistochronic motion of the Chaplygin sleigh. *Acta Mech* 2013; 224: 2127-2141.
- [8] Radulović, R, Obradović, A, and Jeremić, B. Analysis of the minimum required coefficient of sliding friction at brachistochronic motion of a nonholonomic mechanical system. *FME Trans* 2014; 42: 201-206.
- [9] Bloch, AM. *Nonholonomic mechanics and control*. Berlin: Springer, 2003.
- [10] Chaplygin, SA. On the theory of motion of nonholonomic systems. The reducing-multiplier theorem, *Math Collect* 1911; 28: 303-314 (English translation by Getling, AV. *Regular Chaotic Dynam* 2008; 13: 369-376).
- [11] Caratheodory, C. Der Schlitten. *ZAMM-Z Angew Math Me* 1933; 13: 71-76.
- [12] Neimark, JuI, and Fufaev, NA. *Dynamics of nonholonomic systems*. (Translations of Mathematical Monographs 33). Providence, RI: AMS, 1972.
- [13] Ruina, A. Non-holonomic stability aspects of piecewise-holonomic systems. *Rep Math Phys* 1998; 42: 91-100.
- [14] Čović, V, Lukačević, M, and Vesković, M. *On brachistochronic motions*. Budapest: Budapest University of Technology and Economics, 2007.
- [15] Soltakhanov, ShKh, Yushkov, MP, and Zegzhda, SA. *Mechanics of non-holonomic systems*. Berlin: Springer, 2009.
- [16] Antunes, ACB, and Sigaud, C. Controlling nonholonomic Chaplygin systems. *Braz J Phys* 2010; 40: 131-140.
- [17] Obradović, A, Šalinić, S, Jeremić, O, et al. On the brachistochronic motion of a variable-mass mechanical system in general force fields. *Math Mech Solids* 2014; 19: 398-410.
- [18] Pontryagin, LS, Boltyanskii, VG, Gamkrelidze, RV, et al. *The mathematical theory of optimal processes*. NJ: Wiley, 1962.
- [19] Leitmann, G. *An Introduction to optimal control*. New York: McGraw-Hill Book Company, 1966.
- [20] Ruskeepää, H. *Mathematica® navigator: Mathematics, statistics, and graphics*. Amsterdam: Academic Press, 2009.

**AQ8**

**Appendix**

Application of the shooting method in solving the two-point boundary-value problem and an intersection of corresponding surfaces (36) and space curves (42)

(\*Numerical data\*)

```
m = 2;
a = 1;
T0 = 200;
k = 1.5;
CC = 2*T0/m;
A = a*k;
```

**AQ6** (\*Estimation of the values of quantities  $\lambda_x$  and  $\lambda_y$ \*)

```
nn = 1/sqrt[CC];
nn1 = cot[fi]/sqrt[CC];
```

```
Manipulate[{
ss = First[NDSolve[{
```

```
x'[t] == CC*(lx*cos[fi[t]] + ly*sin[fi[t]])*cos[fi[t]],
y'[t] == CC*(lx*cos[fi[t]] + ly*sin[fi[t]])*sin[fi[t]],
fi'[t] == CC*lf[t]/A^2,
lfi'[t] == CC*(lx*cos[fi[t]] + ly*sin[fi[t]])*(lx*sin[fi[t]]-ly*cos[fi[t]]),
x[0] == 0,y[0] == 0,fi[0] == 0,lfi[0] == A*sqrt[1/CC-lx^2]
}],{x,y,fi,lfi},{t,0,tf}],Plot[Evaluate[{{y[t],x[t],fi[t],a,fi}/.ss}],{t,0,tf},PlotRange->{0,3.5}]
}],
```

```
{lx,-nn,nn},{ly,-nn1,nn1},{tf,0,0.6}]
```

```
xx1[lx_?NumberQ,ly_?NumberQ,tf_?NumberQ]:=
```

```
First[x[tf]/.NDSolve[{
```

```
x'[t] == CC*(lx*cos[fi[t]] + ly*sin[fi[t]])*cos[fi[t]],
y'[t] == CC*(lx*cos[fi[t]] + ly*sin[fi[t]])*sin[fi[t]],
fi'[t] == CC*lf[t]/A^2,
lfi'[t] == CC*(lx*cos[fi[t]] + ly*sin[fi[t]])*(lx*sin[fi[t]]-ly*cos[fi[t]]),
x[0] == 0,y[0] == 0,fi[0] == 0,lfi[0] == A*sqrt[1/CC-lx^2]
```

```
},{x,y,fi,lfi},{t,0,tf}]
```

```
xx2[lx_?NumberQ,ly_?NumberQ,tf_?NumberQ]:=
```

```
First[y[tf]/.NDSolve[{
```

```
x'[t] == CC*(lx*cos[fi[t]] + ly*sin[fi[t]])*cos[fi[t]],
y'[t] == CC*(lx*cos[fi[t]] + ly*sin[fi[t]])*sin[fi[t]],
fi'[t] == CC*lf[t]/A^2,
lfi'[t] == CC*(lx*cos[fi[t]] + ly*sin[fi[t]])*(lx*sin[fi[t]]-ly*cos[fi[t]]),
x[0] == 0,y[0] == 0,fi[0] == 0,lfi[0] == A*sqrt[1/CC-lx^2]
```

```
},{x,y,fi,lfi},{t,0,tf}]
```

xx3[lx\_?NumberQ,ly\_?NumberQ,tf\_?NumberQ]: =

First[fi[tf]/.NDSolve[{

x'[t] = CC\*(lx\*cos[fi[t]] + ly\*sin[fi[t]])\*cos[fi[t]],  
 y'[t] = CC\*(lx\*cos[fi[t]] + ly\*sin[fi[t]])\*sin[fi[t]],  
 fi'[t] = CC\*lf[t]/A^2,  
 lfi'[t] = CC\*(lx\*cos[fi[t]] + ly\*sin[fi[t]])\*(lx\*sin[fi[t]]-ly\*cos[fi[t]]),  
 x[0] = 0,y[0] = 0,fi[0] = 0,lfi[0] = A\*sqrt[1/CC-lx^2]  
 },{x,y,fi,lfi},{t,0,tf}]

(\*Solutions of corresponding TPBVP are determined in the manner as follows\*)

FindRoot[{xx1[lx,ly,tf] = xf,xx2[lx,ly,tf] = yf,xx3[lx,ly,tf] = fif},{lx, lx\*},{ly,ly\*},{tf, tf\*}]

(\*where xf, yf and fif are defined final values of the edge state coordinates, whereas lx\*,ly\*and tf\*are visually estimated values of the crossing points coordinates from Figures 3, 9, 14 and 19\*)

(\*Surfaces (36) can be numerically represented as follows\*)

xx11[lx\_,ly\_,tf\_] := xx1[lx,ly,tf]-xf;  
 xx22[lx\_,ly\_,tf\_] := xx2[lx,ly,tf]-yf;  
 xx33[lx\_,ly\_,tf\_] := xx3[lx,ly,tf]-fif;

(\*whereas the intersection of corresponding space curves (42), whose results are shown in Figures 3, 9, 14 and 19, can be defined as\*)

Show[ContourPlot3D[xx11[lx,ly,tf] = 0,{lx,-nn,nn},{ly,-nn1,nn1},{tf,0,0.6},AxesLabel->{Subscript[λ,x],Subscript[λ,y],Subscript[t,f]},LabelStyle->Directive[12],MeshFunctions->{Function[{lx,ly,tf},xx22[lx,ly,tf]],MeshStyle->{{Thick,Blue}},Mesh->{{0}},ContourStyle->None,BoxRatios->{1,1,1}],  
 ContourPlot3D[xx11[lx,ly,tf] = 0,{lx,-nn,nn},{ly,-nn1,nn1},{tf,0,0.6},AxesLabel->{Subscript[λ,x],Subscript[λ,y],Subscript[t,f]},LabelStyle->Directive[12],MeshFunctions->{Function[{lx,ly,tf},xx33[lx,ly,tf]],MeshStyle->{{Thick,Red}},Mesh->{{0}},ContourStyle->None,BoxRatios->{1,1,1}]

(\*Intersection of corresponding surfaces (36), whose results are shown in Figures 2, 8, 13 and 18, can be defined as\*)

Show[{ContourPlot3D[xx1[lx,ly,tf] = xf,{lx,-nn,nn},{ly,-nn1,nn1},{tf,0,0.6},AxesLabel->{Subscript[λ,x],Subscript[λ,y],Subscript[t,f]},LabelStyle->Directive[12],ContourStyle->Red,Mesh->None,BoxRatios->{1,1,1}],  
 ContourPlot3D[xx2[lx,ly,tf] = yf,{lx,-nn,nn},{ly,-nn1,nn1},{tf,0,0.6},AxesLabel->{Subscript[λ,x],Subscript[λ,y],Subscript[t,f]},LabelStyle->Directive[12],ContourStyle->Blue,Mesh->None,BoxRatios->{1,1,1}],  
 ContourPlot3D[xx3[lx,ly,tf] = fif,{lx,-nn,nn},{ly,-nn1,nn1},{tf,0,0.6},AxesLabel->{Subscript[λ,x],Subscript[λ,y],Subscript[t,f]},LabelStyle->Directive[12],ContourStyle->Green,Mesh->None,BoxRatios->{1,1,1}]}